

Calculation of space debris distribution using quantum gravity theory with ultimate acceleration

Huaiyang Cui

Department of Physics, Beihang University, Beijing, 100191, China

Email: hycui@buaa.edu.cn

(June 1, 2022)

Abstract: It was found that ultimate acceleration can enhance the quantum gravity effects for test. If there is an ultimate acceleration β , nobody's acceleration can exceed this limit β , in the solar system, $\beta=2.961520e+10(m/s^2)$. Because this ultimate acceleration is a large number, any effect connecting to β will become easy to test, including quantum gravity test. As an application, the quantum gravity theory with the ultimate acceleration provides a useful formula to calculate the space debris distribution around the earth, in this paper the calculation results agree well with the experimental observation which are a set of measurements by incoherent scattering radar of EISCAT in the Arctic circle. Using the same approach, the radius of the Sun is calculated out to be $r=7e+8$ (m) with a relative error 0.72%; the radius of the Earth is calculated out to be $r=6.4328e+6$ (m) with a relative error 0.97%.

1. Introduction

In general, some quantum gravity proposals [1,2] are extremely hard to test in practice, as quantum gravitational effects are appreciable only at the Planck scale [3]. It was found that ultimate acceleration can enhance the quantum gravity effects for test. If there is an ultimate acceleration β , nobody's acceleration can exceed this limit β , in the solar system, $\beta=2.961520e+10(m/s^2)$. Because this ultimate acceleration is a large number, any effect connecting to β will become easy to test, including quantum gravity test. As an application, the quantum gravity theory with the ultimate acceleration provides a useful formula to calculate the space debris distribution around the earth, in this paper the calculation results agree well with the experimental observation.

With the increasing frequency of human space activities, the impact and harm of space debris are becoming more and more obvious [16,17]. The monitoring and early warning of space debris have gradually been widely investigated [18,19,20]. The Arctic is a key area for space debris monitoring. At present, incoherent scattering radar is the most powerful ground-based ionospheric monitoring means in the world. It mainly studies the ionospheric space environment information by receiving the backscattered echo of transmitted wave. Since the 1960s, more than 10 sets of incoherent scattering radars have been built, mainly by the American and European incoherent scattering radar Scientific Association (EISCAT). The observational data source used in this paper is a set of measurements by incoherent scattering radar of EISCAT in the Arctic circle, with the operating frequency of 500MHz (i.e. ESR radar) [21-25].

2. How to connect quantum gravity with the ultimate acceleration

In the relativity, the speed of light c is an ultimate speed, nobody's speed can exceed this limit c . The relativistic velocity u of a particle in the coordinate system $(x_1, x_2, x_3, x_4=ict)$ satisfies

$$u_1^2 + u_2^2 + u_3^2 + u_4^2 = -c^2 . \quad (1)$$

No matter what particles (electrons, molecules, neutrons, quarks), their 4-vector velocities all have the same magnitude: $|u|=ic$. All particles gain **equality** because of the same magnitude of their 4-velocity u . The acceleration a of the particle is given by

$$a_1^2 + a_2^2 + a_3^2 = a^2; \quad (a_4 = 0; \quad \because x_4 = ict) \quad (2)$$

Assume that particles have an ultimate acceleration β as limit, no particle can exceed this acceleration limit β . Subtracting the both sides of the above equation by β^2 , we have

$$a_1^2 + a_2^2 + a_3^2 - \beta^2 = a^2 - \beta^2; \quad a_4 = 0 \quad (3)$$

It can be rewritten as

$$[a_1^2 + a_2^2 + a_3^2 + 0 + (i\beta)^2] \frac{1}{1 - a^2 / \beta^2} = -\beta^2 \quad (4)$$

Now, the particle subjects to an acceleration whose five components are specified by

$$\begin{aligned} \alpha_1 &= \frac{a_1}{\sqrt{1 - a^2 / \beta^2}}; & \alpha_2 &= \frac{a_2}{\sqrt{1 - a^2 / \beta^2}}; \\ \alpha_3 &= \frac{a_3}{\sqrt{1 - a^2 / \beta^2}}; & \alpha_4 &= 0; & \alpha_5 &= \frac{i\beta}{\sqrt{1 - a^2 / \beta^2}}; \end{aligned} \quad (5)$$

where α_5 is the newly defined acceleration in five dimensional space-time $(x_1, x_2, x_3, x_4=ict, x_5)$. Thus, we have

$$\alpha_1^2 + \alpha_2^2 + \alpha_3^2 + \alpha_4^2 + \alpha_5^2 = -\beta^2; \quad \alpha_4 = 0 \quad (6)$$

It means that the magnitude of the newly defined acceleration α for every particle takes the same value: $|\alpha|=i\beta$ (constant imaginary number).

How to resolve the velocity u and acceleration α into x, y and z components? In realistic world, a hand can rotate a ball moving around a circular path at constant speed v with constant centripetal acceleration a , as shown in Fig.1(a).

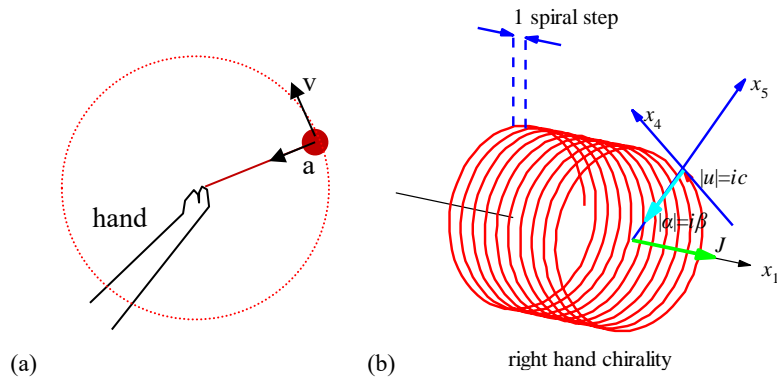


Fig.1 (a) A hand rotates a ball moving around a circular path at constant speed v with constant centripetal acceleration a . (b) The particle moves along the x_1 axis with the constant speed $|u|=ic$ in the u direction and constant centripetal force in the x_5 axis at the radius iR (imaginary number).

```
<Clet2020 Script>/[26]
double D[100],S[2000];int i,j,R,X,N;
int main(){R=50;X=50;N=600;D[0]=-50;D[1]=0;D[2]=0;D[3]=X;D[4]=0;D[5]=0;D[6]=-50;D[7]=R;D[8]=0;
D[9]=600;D[10]=10;D[11]=R;D[12]=0;D[13]=3645;
Lattice(SPIRAL,D,S);SetViewAngle(0,80,-50);DrawFrame(FRAME NULL,1,0xfffff);
Draw("LINE,0,2,XYZ,0",-150,0,0,-50,0,0");Draw("ARROW,0,2,XYZ,10",50,0,0,150,0,0);
SetPen(2,0xff0000);Plot("POLYLINE,0,600,XYZ",S[9]);i=9+3*N-6;Draw("ARROW,0,2,XYZ,10",S[i]);
TextHang(S[i],S[i+1],S[i+2]," #if|u|=ic#t");TextHang(150,0,0," #ifx#sd1#t");SetPen(2,0x005fff);
Draw("LINE,1,2,XYZ,8",-50,0,50,-50,0,100);Draw("LINE,1,2,XYZ,8",-40,0,50,-40,0,100);
Draw("ARROW,0,2,XYZ,10",-80,0,100,-50,0,100);Draw("ARROW,0,2,XYZ,10",-10,0,100,-40,0,100);
TextHang(-50,0,110,"1 spiral step");i=9+3*N;S[i]=50;S[i+1]=10;S[i+2]=10;
Draw("ARROW,0,2,XYZ,10",50,0,0,50,80,80);TextHang(50,80,80," #ifx#sd5#t");
Draw("ARROW,0,2,XYZ,10",50,72,0,50,0,72);TextHang(50,0,72," #ifx#sd4#t");
SetPen(3,0x00ffff);Draw("ARROW,0,2,XYZ,15",S[i-3]);TextHang(S[i],S[i+1],S[i+2]," #if|alpha|=i|beta#t");
SetPen(3,0x00ff00);Draw("ARROW,0,2,XYZ,15",50,0,0,120,0,0);TextHang(110,5,5," #ifj#t");
TextHang(-60,0,-80," right hand chirality");#v07=?>A
```

In analogy with the ball in a circular path, consider a particle in one dimensional motion along the x_1 axis at the speed v , in the Fig.1(b) it moves with the constant speed $|u|=ic$ almost along the x_4 axis and slightly along the x_1 axis, and the constant centripetal acceleration $|\alpha|=i\beta$ in the x_5 axis at the constant radius iR (imaginary number); the coordinate system $(x_1, x_4=ict, x_5=iR)$ establishes a cylinder coordinate system in which this particle moves spirally at the speed v along the x_1 axis. According to usual centripetal acceleration formula, the acceleration in the x_4 - x_5 plane is given by

$$i\beta = \frac{|u|^2}{iR} = -\frac{c^2}{iR} = i\frac{c^2}{R} . \quad (7)$$

Therefore, the track of the particle in the cylinder coordinate system $(x_1, x_4=ict, x_5=iR)$ forms a shape, called as **acceleration-roll**. The faster the particle moves, the longer the spiral step is.

As like a steel spring which contains elastic wave, the track in the acceleration-roll in Fig.1(b) can be described by a wave function whose phase changes 2π for one spiral step. The wave function phase changes 2π for one spiral circumferences $2\pi(iR)$, and the small displacement of the particle on the spiral track is $|u|d\tau=icd\tau$ in the 4-vector u direction, thus this wave phase along the spiral track is evaluated by

$$phase = \int_0^\tau \frac{2\pi}{2\pi(iR)} icd\tau = \int_0^\tau \frac{c}{R} d\tau . \quad (8)$$

Substituting the radius R into it, the wave function ψ is given by

$$\psi = \exp(-i \cdot phase) = \exp(-i \int_0^\tau \frac{c}{R} d\tau) = \exp(-i \frac{\beta}{c} \int_0^\tau d\tau) . \quad (9)$$

In the theory of relativity, we known that the integral along $d\tau$ needs to transform into realistic line integral, that is

$$\begin{aligned} d\tau &= -c^2 \frac{d\tau}{-c^2} = (u_1^2 + u_2^2 + u_3^2 + u_4^2) \frac{d\tau}{-c^2} \\ &= (u_1 dx_1 + u_2 dx_2 + u_3 dx_3 + u_4 dx_4) \frac{1}{-c^2} . \end{aligned} \quad (10)$$

Therefore, the wave function ψ is evaluated by

$$\begin{aligned}\psi &= \exp\left(-i \frac{\beta}{c} \int_0^\tau d\tau\right) \\ &= \exp\left(i \frac{\beta}{c^3} \int_0^x (u_1 dx_1 + u_2 dx_2 + u_3 dx_3 + u_4 dx_4)\right)\end{aligned}\quad (11)$$

This wave function may have different explanations, depending on the particle under investigation. If the β is replaced by the Planck constant, the wave function of electrons is given by

$$\begin{aligned}\text{assume: } \beta &= \frac{mc^3}{\hbar} \\ \psi &= \exp\left(\frac{i}{\hbar} \int_0^x (mu_1 dx_1 + mu_2 dx_2 + mu_3 dx_3 + mu_4 dx_4)\right)\end{aligned}\quad (12)$$

where $mu_4 dx_4 = -Edt$, it strongly suggests that the wave function is just the **de Broglie's matter wave** [4,5,6]. In Fig.1(b), the acceleration-roll of particle moves with two distinctions: right-hand chirality and left-hand chirality. The direction of the angular momentum J would be slightly different from the advance x_1 due to spiral precession. It is easy to calculate the ultimate acceleration β , the radius R and the angular momentum J in the plane x_4 - x_5 for spiraling electron as

$$\begin{aligned}\beta &= \frac{c^3 m}{\hbar} = 2.327421e+29 \text{ (M/s}^2\text{)} \\ R &= \frac{c^2}{\beta} = 3.861593e-13 \text{ (M)} \\ J &= \pm m |u| iR = \mp \hbar\end{aligned}\quad (13)$$

```
<Clet2020 Script>/[26]
double beta,R,J,m,D[10];char str[200];
int main(){m=ME;beta=SPEEDC*SPEEDC*SPEEDC*m/PLANCKBAR;
R=SPEEDC*SPEEDC/beta;J=PLANCKBAR;Format(str,"beta=%e, #nR=%e, #nJ=%e",beta,R,J);
TextAt(50,50,str);ClipJob(APPEND,str);}#v07=#t
```

The wave function ψ in Eq.(11) is a pure geometry wave. Considering planets in the solar system, no Planck constant can be involved. In a many-body system with the total mass M , the ultimate acceleration can be rewritten in terms of **Planck-constant-like constant h** as

$$\begin{aligned}\text{assume: } \beta &= \frac{c^3}{hM} \\ \psi &= \exp\left(\frac{i}{hM} \int_0^x (u_1 dx_1 + u_2 dx_2 + u_3 dx_3 + u_4 dx_4)\right)\end{aligned}\quad (14)$$

The constant h will be determined by experimental observations. In next section we shall try to use this wave function as the planetary scale waves in the solar system to explain quantum gravity effects for the planets and satellites, the wave function is called as the **acceleration-roll wave**.

Tip: actually, ones cannot get to see the acceleration-roll of particle in the relativistic space-time ($x_1, x_2, x_3, x_4 = ict$) ; only get to see it in the cylinder coordinate system ($x_1, x_4 = ict, x_5 = iR$).[28]

3. The acceleration-roll wave in planetary systems

In the Bohr's orbit model for planets or satellites, as shown in Fig.2, the circular quantization condition is in terms of acceleration-roll wave given by

$$\left. \begin{array}{l} \frac{\beta}{c^3} \oint_L v_l dl = 2\pi n \\ v_l = \sqrt{\frac{GM}{r}} \end{array} \right\} \Rightarrow \sqrt{r} = \frac{c^3}{\beta\sqrt{GM}} n; \quad n = 0, 1, 2, \dots \quad (15)$$

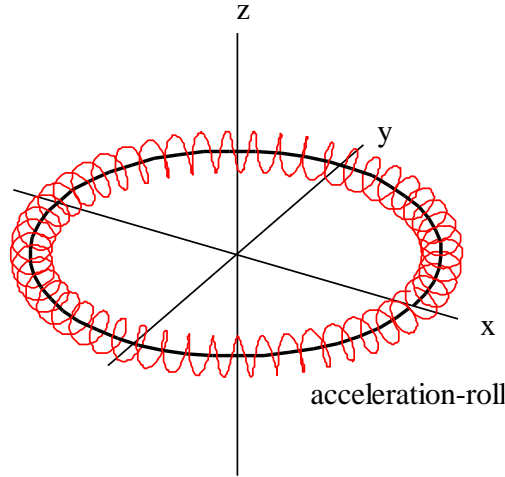


Fig.2 A planet 2D orbit around the sun, an acceleration-roll winding around the planet.

```
<Clet2020 Script>[[26]
int i,j,k; double r,rot,x,y,z,D[20],F[20],S[200];
int main(){SetViewAngle("temp0,theta60,phi-30");
DrawFrame(FRAME LINE,1,0xaffaf);r=80;Spiral(); TextHang(r,-r,0,"acceleration-roll");
r=110;TextHang(r,0,0,"x");TextHang(0,r,0,"y");TextHang(0,0,r,"z");}
Spiral(){r=80;j=10;rot=j/r;k=2*PI/rot+1;
for(i=0;i<k;i+=1){D[0]=x;D[1]=y;D[2]=z;D[6]=x;D[7]=y;D[8]=r;
x=r*cos(rot*i);y=r*sin(rot*i);z=0;if(i==0) continue;
SetPen(2,0x00);F[0]=D[0];F[1]=D[1];F[2]=x;F[3]=y;Draw("LINE,0.2,XY",F);SetPen(1,0xff0000);
D[3]=x;D[4]=y;D[5]=z; D[9]=40;D[10]=10;D[11]=8;D[12]=0;D[13]=360;
Lattice(SPIRAL,D,S);Plot("POLYLINE,0.40,XYZ",S[9]);}
}#v07=?>A
```

The solar system, Jupiter's satellites, Saturn's satellites, Uranus' satellites, Neptune's satellites as five different many-body systems are investigated with the Bohr's orbit model. After fitting observational data as shown in Fig.3, their ultimate accelerations are obtained in Table 1. The predicted quantization-blue-lines in Fig.3(a), Fig.3(b), Fig.3(c), Fig.3(d) and Fig.3(e) agrees well with experimental observations for those inner constituent planets or satellites.

Beside every β , our interest shifts to the constant h in Table 1, which is defined as

$$h = \frac{c^3}{M\beta} \Rightarrow \sqrt{r} = h\sqrt{\frac{M}{G}} n \quad (16)$$

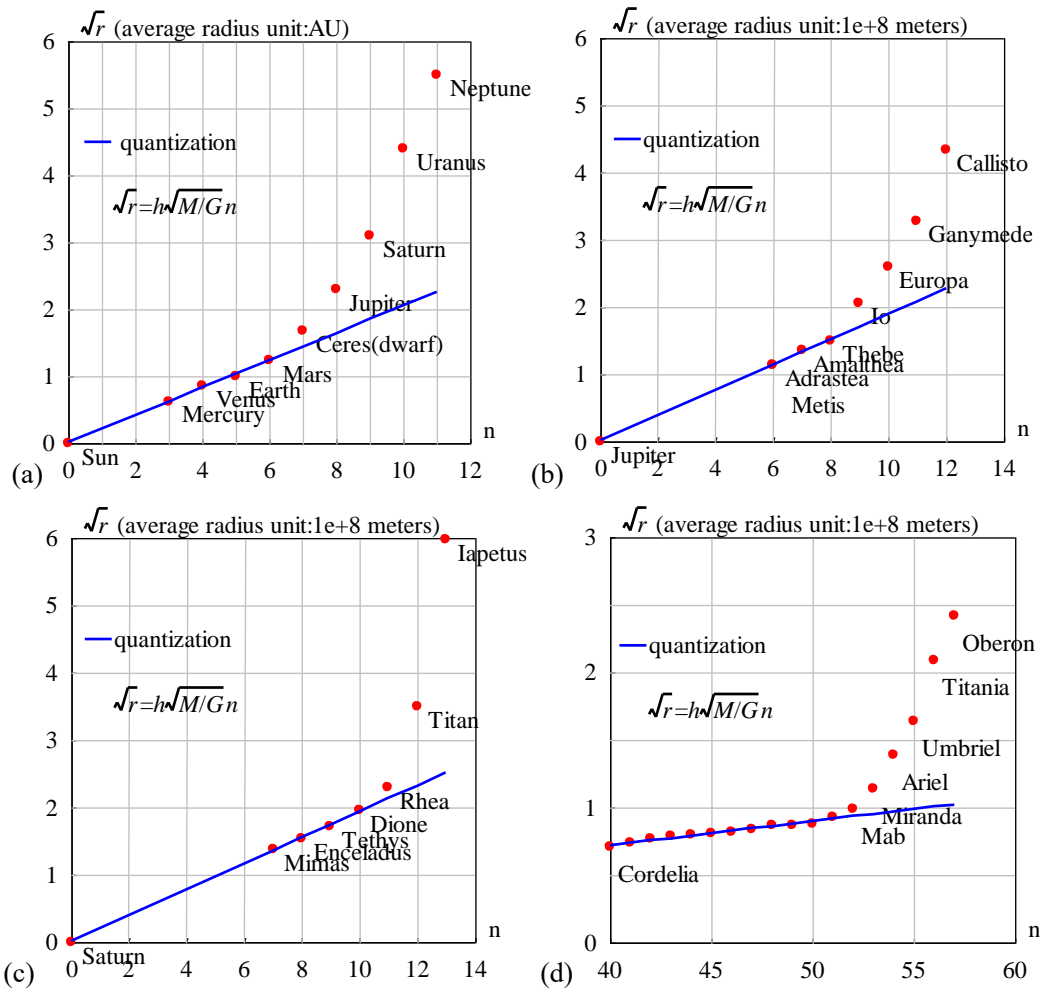
In a many-body system with the total mass M , a constituent particle has the mass m and moves at the speed v , it is easy to find that the wavelength of de Broglie's matter wave should be modified for planets and satellites as

$$\lambda = \frac{2\pi\hbar}{mv} \Rightarrow \text{modify} \Rightarrow \lambda = \frac{2\pi h M}{v} \quad (17)$$

where h is a **Planck-constant-like constant**. Usually the total mass M is approximately equal to the central-star's mass. It is found that this modified matter wave works for quantizing orbits correctly in Fig.3 [28,29]. The key point is that the various systems have almost same Planck-constant-like constant h in Table 1 with a mean value of $3.51\text{e-}16 \text{ m}^2\text{s}^{-1}\text{kg}^{-1}$, at least have the same magnitude! The acceleration-roll wave is a generalized matter wave as a planetary scale wave.

Table 1 Planck-constant-like constant h in various systems, N is constituent particle number with smaller inclination.

system	N	M/M_{earth}	$\beta \text{ (m/s}^2\text{)}$	$h \text{ (m}^2\text{s}^{-1}\text{kg}^{-1}\text{)}$	Prediction
Solar planets	9	333000	$2.961520\text{e}+10$	$4.574635\text{e-}16$	Fig.3(a)
Jupiter' satellites	7	318	$4.016793\text{e}+13$	$3.531903\text{e-}16$	Fig.3(b)
Saturn's satellites	7	95	$7.183397\text{e}+13$	$6.610920\text{e-}16$	Fig.3(c)
Uranus' satellites	18	14.5	$1.985382\text{e}+15$	$1.567124\text{e-}16$	Fig.3(d)
Neptune 's satellites	7	17	$2.077868\text{e}+15$	$1.277170\text{e-}16$	Fig.3(e)



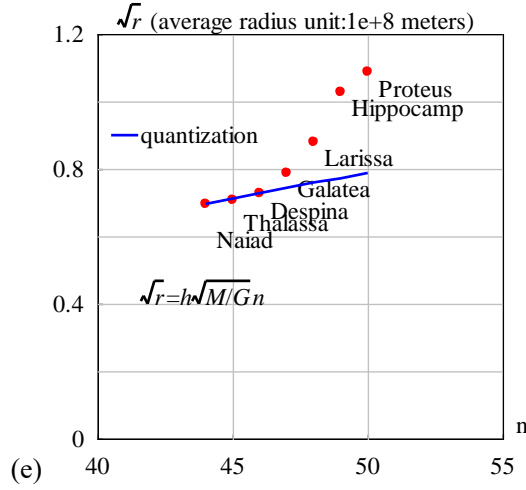


Fig.3 The orbital radii are quantized for inner constituents. (a) the solar system with $h=4.574635e-16$ ($m^2s^{-1}kg^{-1}$). The relative error is less than 3.9%. (b) the Jupiter system with $h=3.531903e-16$ ($m^2s^{-1}kg^{-1}$). Metis and Adrastea are assigned the same quantum number for their almost same radius. The relative error is less than 1.9%. (c) the Saturn system with $h=6.610920e-16$ ($m^2s^{-1}kg^{-1}$). The relative error is less than 1.1%. (d) the Uranus system with $h=1.567124e-16$ ($m^2s^{-1}kg^{-1}$). $n=0$ is assigned to the Uranus. The relative error is less than 2.5%. (e) the Neptune system with $h=1.277170e-16$ ($m^2s^{-1}kg^{-1}$). $n=0$ is assigned to the Neptune. The relative error is less than 0.17%.

In Fig.3(a), the blue straight line expresses the linear regression relation among the Sun, Mercury, Venus, Earth and Mars, their quantization parameters are $hM=9.098031e+14(m^2/s)$. The ultimate acceleration is $\beta=2.961520e+10$ (m/s^2). Where, $n=3,4,5,..$ were assigned to solar planets, the sun was assigned a quantum number $n=0$ because the sun is in the **central state**.

4. Optical model of solar central state

The acceleration-roll wave as the generalized matter wave is given by

$$\psi = \exp\left(\frac{i}{hM} \int_0^x v_l dl\right); \quad \lambda = \frac{2\pi hM}{v_l} \quad (18)$$

In a central state $n=0$, if the coherent length of the acceleration-roll wave is long enough, its head may overlap with its tail when the particle moves in a closed orbit in the space time, as shown in Fig.4, the interference of the acceleration-roll wave between its head and tail will occur in the overlapping zone. Because the acceleration-roll wave winds around the time axis and overlaps itself, the overlapped wave is given by

$$\psi(r) = 1 + e^{i\delta} + e^{i2\delta} + \dots + e^{i(N-1)\delta} = \frac{1 - \exp(iN\delta)}{1 - \exp(i\delta)} \quad (19)$$

$$\delta(r) = \frac{1}{hM} \oint_L (v_l) dl = \frac{2\pi\omega r^2}{hM}$$

where N is the overlapping number which is determined by the coherent length of the acceleration-roll wave, δ is the phase difference after one orbital motion, ω is the angular speed of the sun rotation. The above equation is a multi-slit interference formula in optics, for a larger N it is called as the

Fabry-Perot interference formula.

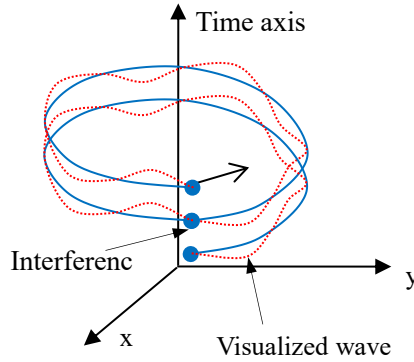


Fig.4 The head of the acceleration-roll wave may overlap with its tail.

The acceleration-roll wave function ψ needs a further explanation. In quantum mechanics, $|\psi|^2$ equals to the probability of finding an electron due to Max Burn's explanation; in astrophysics, $|\psi|^2$ equals to the probability of finding a nucleon (proton or neutron) *averagely in astronomic scale*, because all mass is mainly made of nucleons, we have

$$|\psi|^2 \propto \text{nucleon_density} . \quad (20)$$

It follows from the multi-slit interference formula that the interference intensity at close to maxima is proportion to N^2 , that is

$$N^2 = \frac{|\psi(0)_{\text{multi-wavelet}}|^2}{|\psi(0)_{\text{one-wavelet}}|^2} . \quad (21)$$

What matter plays the role of "one-wavelet" in the solar core or Earth core? We choose vapor above the sea on the earth surface as the "reference matter: one-wavelet". Thus, the overlapping number N is estimated by

$$N^2 = \frac{|\psi(0)_{\text{multi-wavelet}}|^2}{|\psi(0)_{\text{one-wavelet}}|^2} \approx \frac{\text{core_nucleon_density}_{r=0}}{\text{vapor_above_sea_density}} . \quad (22)$$

Although today there is not vapor on the solar surface, the solar core has a density of $1.5e+5 \text{ kg/m}^3$ [31], comparing to the vapor density 1.29 kg/m^3 on the earth, the solar overlapping number N is still estimated as $N=341$. The Earth core density is $5.53e+3 \text{ kg/m}^3$, the Earth's overlapping number N is estimated as $N=65$.

For the Sun, Earth and Mars, their central densities and their reference matter density are given in the Table 1. Thus, their overlapping numbers are estimated also in this table.

Table 1 Estimating the overlapping number N by comparing solid core and reference matter, regarding protons and neutrons as basis particles.

object	Solid core, density (kg/m ³)	Reference matter, density (kg/m ³)	Overlapping number N	β (m/s ²)
Sun	1.5e+5 (max.)	1.29 (vapor above the sea)	341	2.961520e+10
Earth	5530	1.29 (vapor above the sea)	65	1.377075e+14
Mars	3933.5	1.29 (vapor above the sea)	55	2.581555e+15
Jupiter	1326			4.016793e+13

Saturn	687			7.183397e+13
Uranus	1270			1.985382e+15
Neptune	1638			2.077868e+15
Alien-planet	5500	1.29(has water on the surface)	65	

Sun's rotation angular speed at the equator is known as $\omega=2\pi/(25.05*24*3600)$, unit s^{-1} . Its mass $1.9891e+30$ (kg), radius $6.95e+8$ (m), mean density 1408 (kg/m^3), the solar core has a maximum density of $1.5e+5kg/m^3$ [31], the ultimate acceleration $\beta=2.961520e+10$ (m/s^2), the constant $hM=9.100745e+14$ (m^2/s). According to the $N=341$, the matter distribution of the $|\psi|^2$ is calculated out in Fig.5, it agrees well with the general description of the sun's interior. The radius of the Sun is calculated out to be $r=7e+8$ (m) with a relative error 0.72% in the Fig.5, it indicates that the sun radius strongly depends on the sun self-rotation.

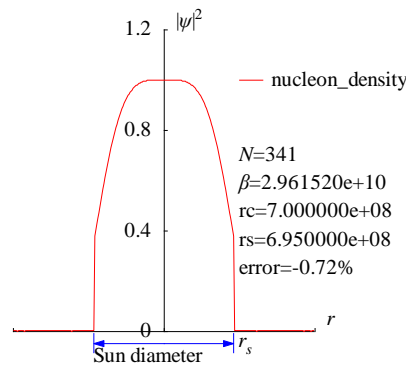


Fig.5 The matter distribution $|\psi|^2$ around the Sun has been calculated in radius direction.

```
<Clet2020 Script>//[26]
int i,j,k,m,n,N,nP[10];
double beta,H,B,M,r,r_unit,x,y,z,delta,D[1000],S[1000],a,b,rs,rc,rot,atm_height; char str[100];
main(){k=150;rs=6.95e8;rc=0;x=25.05;rot=2*PI/(x*24*3600);n=0; N=341;
beta=2.961520e10;H=SPEEDC*SPEEDC*SPEEDC/beta;M=1.9891E30; atm_height=2e6; r_unit=1E7;
b=PI/(2*PI*rot*rs*rs/H);
for(i=-k;i<k;i+=1){r=abs(i)*r_unit;
if(r<rs+atm_height) delta=2*PI*rot*r/H; else delta=2*PI*sqrt(GRAVITYC*M*r)/H;//around the star
y=SumJob("SLIT_ADD,@N,@delta",D); y=y/(N*N);
S[n]=i;S[n+1]=y; if(i>0 && rc==0 && y<0.001) rc=r;D[n]=i;D[n+1]=z;n+=2;}
SetAxis(X_AXIS,-k,0,k,"#ifr; ;");SetAxis(Y_AXIS,0,0,1.2,"#ifpsi#su2#t;0;0.4;0.8;1.2;");
DrawFrame(FRAME_SCALE,1,0xaffaf); z=100*(rs-rc)/rs;
SetPen(1,0xff0000);Polyline(k+k,S,k/2,1," nucleon_density"); SetPen(1,0x0000ff); //Polyline(k+k,D);
//Draw("LINE,0,2,XY,0","20,0.5,60,0.6");TextHang(60,0.6,0,"core");
r=rs/r_unit;y=-0.05;D[0]=-r;D[1]=y;D[2]=r;D[3]=y; Draw("ARROW,3,2,XY,10,100,10,10,");D);
Format(str,"#ifN#t=%d#n#ifbeta#t=%e#nrc=%e#nrs=%e#nerror=%,2f%",N,beta,rc,rs,z);
TextHang(k/2,0.7,0,str);TextHang(r+5,y/2,0,"#ifr#sds#t");TextHang(-r,y+0,"Sun diameter");
}#v07=?>A
```

5. Earth central state and space debris distribution

Applying the acceleration-roll way to the Moon, as illustrated in Fig.6(a), the Moon has been assigned a quantum number of $n=2$ in author's early study [28]. According to Eq.(15), the ultimate acceleration is fitted out to be $\beta=1.377075e+14$ (m/s^2) in the Earth system. Another consideration is to take the quasi-satellite's perigee into account, for the moon and 2004_GU9 etc., as shown in Fig.6(b), but this consideration requires further understanding to its five quasi-satellites [28].

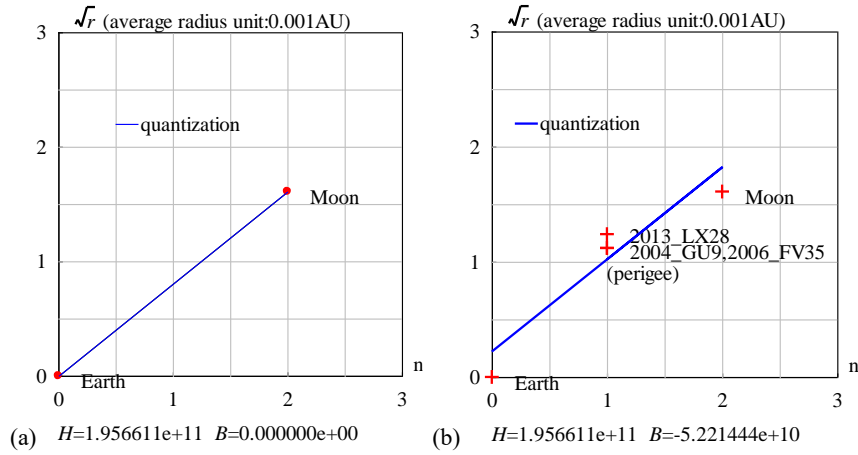


Fig.6 orbital quantization for moon and quasi-satellites to the Earth, $H=hM$.

```
<Clet2020 Script>/[26]
char str[200];int i,j,k,N,nP[10]; double x,y,z,M,r_unit,a,b,B,H,r_ave[20],dP[10],D[1000];
double orbit[10]={0,2.57,0,}; double e[10]={0, 0.0549,0,0,0,0,0,0,0,};
int qn[10]={0,2,3,4,5,6,7,8,9,10,};
char Stars[100]="Earth;Moon;";
int main(){ N=2; M=5.97237E24; r_unit=1.495978707e8;
for(i=0;i<N;i+=1) {x=orbit[i];y=e[i]; z=x*(1+sqrt(1-y*y))/2; r_ave[i]=z;//average_radius
D[i+1]=qn[i];D[i+1+1]=sqrt(z); }
DataJob("REGRESSION,2",D,dP);b=dP[0];a=dP[1];
SetAxis(X_AXIS,0,0,3,"n;0;1;2;3;");
SetAxis(Y_AXIS,0,0,3,"#if#r#t#t (average radius unit:0.001AU);0;1;2;3;");
DrawFrame(0x0166,1,0xaffaf); Polyline(N,D);
SetPen(2,0xff0000); Plot("OVALFILL,0,2,XY,3,3","D");
for(i=0;i<N;i+=1) {nP[0]=TAKE;nP[1]=i;TextJob(nP,Stars,str);x=qn[i]+0.2;y=sqrt(orbit[i])-0.05;TextHang(x,y,0,str);}
x=GRAVITYC*M*r_unit;z=sqrt(x);H=z*a;B=-z*b;
TextAt(100,450,"#if#t=#e #ifB#t=#e",H,B);
for(i=0;i<N;i+=1) {y=b+a*qn[i];D[i+1]=qn[i];D[i+1+1]=y;}
SetPen(1,0x0000ff);Polyline(N,D,0,5,2,2,"quantization");//check
}#v07=?>A
```

Now let us talk about the central state of the earth, the earth's rotation angular speed is known as $\omega=2\pi/(24*3600)$, unit s^{-1} . Its mass $5.97237e+24$ (kg), radius $6.371e+6$ (m), core density 5530 (kg/m^3), the ultimate acceleration $\beta=1.377075e+14$ (m/s^2), the constant $hM=1.956611e+11$ (m^2/s).

We have estimated that the wave overlapping number in the central state of the earth is $N=65$, the matter distribution $|\psi|^2$ in radius direction is calculated out as shown in Fig.7(a), where the self-rotation near its equator has the period of 24 hours:

$$\delta(r) = \frac{1}{hM} \oint_L (v_l) dl = \frac{2\pi r}{hM} \omega r \quad . \quad (23)$$

There is a central maximum of matter distribution at the earth hart, which gradually decreases to zero near the earth surface, then rises the secondary peaks and attenuates down off. The radius of the earth is calculated out to be $r=6.4328e+6$ (m) with a relative error 0.97% using the interference of its acceleration-roll wave. Space debris over the atmosphere has a complicated evolution [7,8], has itself speed

$$v_l = \sqrt{\frac{GM}{r}}; \quad \delta(r) = \frac{\beta}{c^3} \oint_L (v_l) dl = \frac{2\pi\beta}{c^3} \sqrt{GM} r \quad . \quad (24)$$

The secondary peaks over the atmosphere up to 2000km altitude is calculated out in Fig.7(b) which agrees well with the space debris observations [16]; the peak near 890 km altitude is due principally to the January 2007 intentional destruction of the Fengyun-1C weather spacecraft while the peak centered at approximately 770 km altitude was created by the February 2009 accidental collision of Iridium 33 (active) and Cosmos 2251 (derelict) communication spacecraft [16,18]. The observations based on the incoherent scattering radar EISCAT ESR located at 78°N in Jul. 2006 and in Oct. 2015

[21,22,23] are respectively shown in Fig.7(c) and (d). This prediction to secondary peaks also agrees well with other space debris observations [24,25].

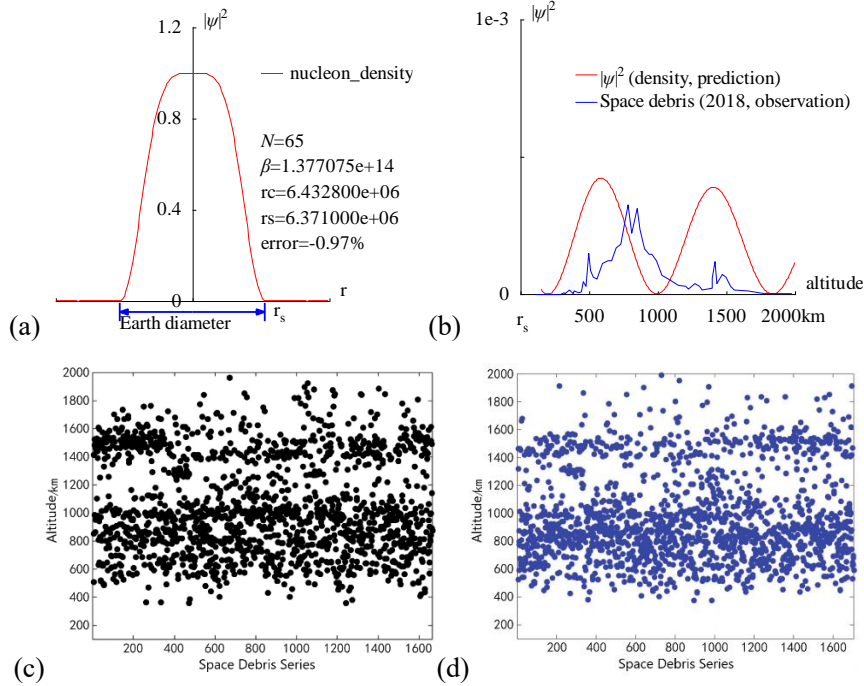


Fig.7 (a) The radius of the Earth is calculated out $r=6.4328e+6$ (m) with a relative error 0.97% by the interference of its acceleration-roll wave; (b) The prediction of the space debris distribution up to 2000km altitude; (c) The space debris distribution in Jul. 2006, Joint observation based on the incoherent scattering radar EISCAT ESR located at 78°N [21]; (d) The space debris distribution in Oct. 2015, Joint observation based on the incoherent scattering radar EISCAT ESR located at 78°N [21].

```
<Clet2020 Script>[[26]
int i,j,k,m,n,N,nP[10];
double H,B,M,v_r,r,AU,r_unit,x,y,z,delta,D[10],S[1000];
double rs,rc,rot,a,b,atm_height,beta; char str[100];
main(){k=80;rs=6.371e6;rc=0;atm_height=1.5e5;n=0; N=65;
beta=1.377075e+14;H=SPEEDC*SPEEDC*SPEEDC/beta;
M=5.97237e24;AU=1.496E11;r_unit=1e-6*AU;
rot=2*PI/(24*60*60);//angular speed of the Earth
for(i=-k;i<k;i+=1) {r=abs(i)*r_unit;
if(r<rs+atm_height) v_r=rot*i*r; else v_r=sqrt(GRAVITYC*M*r);//around the Earth
delta=2*PI*v_r/H; y=SumJob("SLIT_ADD,@N,@delta",D); y=y/(N*N);
if(y>1) y=1; S[n]=i;S[n+1]=y; if(i>0 && rc=0 && y<0.001) rc=r; n+=2;}
SetAxis(X_AXIS,-k,0,k,"r; ;");SetAxis(Y_AXIS,0,0,1.2,"#i|ψ|/su2#t;0;0.4;0.8;1.2;");
DrawFrame(FRAME_SCALE,1,0,0,0,0); x=50; z=100*(rs-rc)/rs;
SetPen(1,0,0,0,0); Polyline(k+k,S,k/2,1,"nucleon_density");
r=rs/r_unit;y=-0.05;D[0]=-r;D[1]=y;D[2]=r;D[3]=y;
SetPen(2,0,0,0,0); Draw("ARROW,3,2,XY,10,100,10,10,"D);
Format(str,"#iN#=#d#n#i#t#=#e#nrc=#e#nrs=#e#nerror=#.2f% ",N,beta,rc,rs,z);
TextHang(k/2,0.7,0,str);TextHang(r+5,y/2,0,"r#sds#t");TextHang(-r,y+y,0,"Earth diameter");
}#v07=?>A
```

```
<Clet2020 Script>[[26]
int i,j,k,m,n,N,nP[10]; double H,B,M,v_r,r,AU,r_unit,x,y,z,delta,D[10],S[10000];
double rs,rc,rot,a,b,atm_height,p,T,R1,R2,R3; char str[100];
int
Debris[96]={110,0,237,0,287,0,317,2,320,1,357,5,380,1,387,4,420,2,440,3,454,14,474,9,497,45,507,26,527,19,557,17,597,34,63,
4,37,664,37,697,51,727,55,781,98,808,67,851,94,871,71,901,50,938,44,958,44,991,37,1028,21,1078,17,1148,10,1202,9,1225,6,
1268,12,1302,9,1325,5,1395,7,1395,18,1415,36,1429,12,1469,22,1499,19,1529,9,1559,5,1656,4,1779,1,1976,1,};
main(){k=80;rs=6.371e6;rc=0;atm_height=1.5e5;n=0; N=65;
H=1.956611e11;M=5.97237e24;AU=1.496E11;r_unit=1e4;
rot=2*PI/(24*60*60);//angular speed of the Earth
b=PI/(2*PI*rot*rs*rs/H); R1=rs/r_unit;R2=(rs+atm_height)/r_unit;R3=(rs+2e6)/r_unit;
for(i=R2;i<R3;i+=1) {r=abs(i)*r_unit; delta=2*PI*sqrt(GRAVITYC*M*r)/H;
y=SumJob("SLIT_ADD,@N,@delta",D); y=1e3*y/(N*N);// visualization scale:1000
if(y>1) y=1; S[n]=i;S[n+1]=y;n+=2;}
SetAxis(X_AXIS,R1,R1,R3,"altitude; r#sds#t;500;1000;1500;2000km :");
SetAxis(Y_AXIS,0,0,1,"#i|ψ|/su2#t;0; ;1e-3;");DrawFrame(FRAME_SCALE,1,0,0,0,0); x=R1+(R3-R1)/5;
SetPen(1,0,0,0,0); Polyline(n/2,S,x,0.8,"#i|ψ|/su2#t (density, prediction)");
for(i=0;i<48;i+=1) {S[i+i]=R1+(R3-R1)*Debris[i+i]/2000; S[i+i+1]=Debris[i+i+1]/300;}
```

```
SetPen(1,0x0000ff);Polyline(48,S,x,0.7,"Space debris (2018, observation) ");
}#v07=?>A
```

6. Mars and Jovian planets

The Mars and its satellites are quantized very well by its ultimate acceleration β as shown in Fig.8(a). Now let us talk about the Mars in the central state with quantum number $n=0$, its ultimate acceleration is $\beta=2.581555e+15(m/s^2)$ in the Mars system. We have estimated the Mars overlapping number $N=55$ in Table 1, the matter distribution $|\psi|^2$ around the Mars can be calculated out in radius direction as shown in Fig.8(b), where the self-rotation at equator has the period of 24 hours.

The radius of the Mars is calculated out as $r=1.6e+6$ (m) with a relative error 52.79%, no further attempt was made to improve the calculation, because of limited knowledge about the Mars history. But one thing is certain, the Mars has frequently bombarded with smaller objects, in fact, consequently with the inclination of 25.2 degrees, so that its self-rotation is unstable or incorrect for its formation in a sense. At very beginning, the Mars self-rotation should have a period of 100 hours. Thanks to the Mars for safeguarding the Earth.

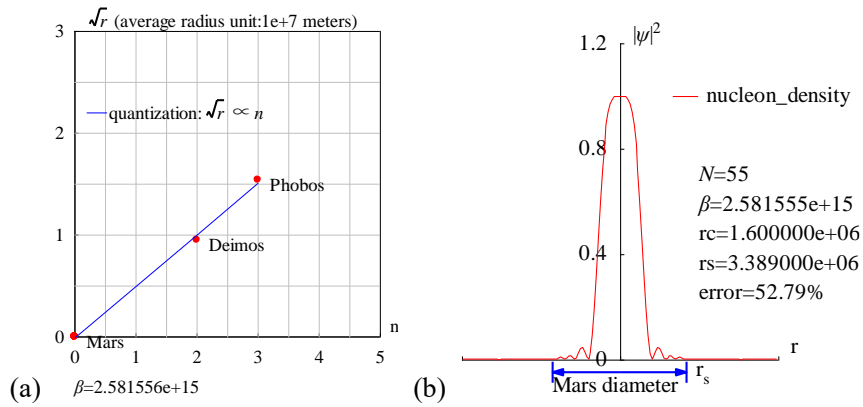


Fig.8 (a)Quantization of Mars and its satellites. (b)The matter distribution $|\psi|^2$ around the Mars has been calculated in radius direction.

```
<Clet2020 Script>//[26]
int i,j,k,m,n,N,nP[10];
double H,B,M,v_r,r,AU,r_unit,x,y,z,delta,D[10],S[1000],F[1000];
double rs,rc,rot,a,b,atm_height,beta; char str[100];
main(){k=80;rs=3.389e6;rc=0;atm_height=10e3;n=0; N=55;
beta=2.581555e+15; H=SPEEDC*SPEEDC*SPEEDC/beta;
M=0.107*5.97237e24; AU=1.496E11;r_unit=1e5;
rot=2*PI/(24*60*60);//angular speed
for(i=-k;i<k;i+=1){r=abs(i)*r_unit;
if(r<rs+atm_height) v_r=rot*r; else v_r=sqrt(GRAVITYC*M/r);//around the star
delta=2*PI*v_r/H;y=SumJob("SLIT_ADD,@N,@delta",D); y=y/(N*N);
if(y>1) y=1; S[n]=i;S[n+1]=y; if(i>0 && rc==0 && y<0.001) rc=r; n+=2;}
SetAxis(X_AXIS,-k,0,k,"r; ;");SetAxis(Y_AXIS,0,0,1.2,"#f|psi#su2#t;0;0.4;0.8;1.2;");
DrawFrame(FRAME_SCALE,1,0,afffaf); x=50;z=100*(rs-rc)/rs;
SetPen(1,0xff0000);Polyline(k+k,S,k/3,1," nucleon_density");
r=rs/r_unit;y=-0.05;D[0]=-r;D[1]=y;D[2]=r;D[3]=y;
SetPen(2,0x0000ff); Draw("ARROW,3,2,XY,10,100,10,10," ,D);
Format(str,"#i#N#t=%d#n#i#f#t=%e#nrc=%e#nrs=%e#nerror=%0.2f% ",N,beta,rc,rs,z);
TextHang(k/2,0.7,0,str);TextHang(r+5,y/2,0,"r#sds#t"); TextHang(-r,y+0,"Mars diameter");
}#v07=?>A
```

In order to extend the quantization rule to the Jovian planets (Jupiter, Saturn, Uranus and Neptune), it is necessary to further study the magnet-like components of gravity [28], the issue beyond the scope of this paper.

7. Discussions

In general, the radius of a planet is determined by the equation of state (EOS) chosen to relate density, pressure, and temperature [9]. D. Valencia et al. presented a model to calculate the relationship between planetary mass, radius, and bulk composition for planets in the 1–10 times earth mass [10,11]. T. Guillot et al. have shown that the evolution of Pegasi planets is mainly driven by processes occurring in their atmosphere and is consequently complex; HD 209458b's large radius cannot be reproduced unless the planet is much younger than is revealed by observations of its parent star [12,13]. Interior dynamics and the belt/zone circulation of giant planet atmospheres were discussed in the literature [14-15]. Therefore, we suggest that the Fabry-Perot interference formula Eq.(19) is a new type of the equation of state (EOS) in terms of the acceleration-roll wave, which is elegant and promising.

A low Earth orbit (LEO) is an Earth-centered orbit with an altitude of 2,000 km or less (approximately one-third of the radius of Earth). Fig.9 shows orbit size comparison of Earth; ISS; Hubble; Iridium; Inner Van Allen belt; GLONASS; GPS; BeiDou; Galileo; Geostationary orbit. The Moon's orbit is around 9 times as large as geostationary orbit. Since the low earth orbit and its nearby orbits are not quantized orbit, the all artificial satellites and space debris under their adaptive force will fall back to the surface of the earth finally, except for the Moon. As we can see so far, the Low Earth orbit (LEO) space is a wild world which bears human's ambitions.

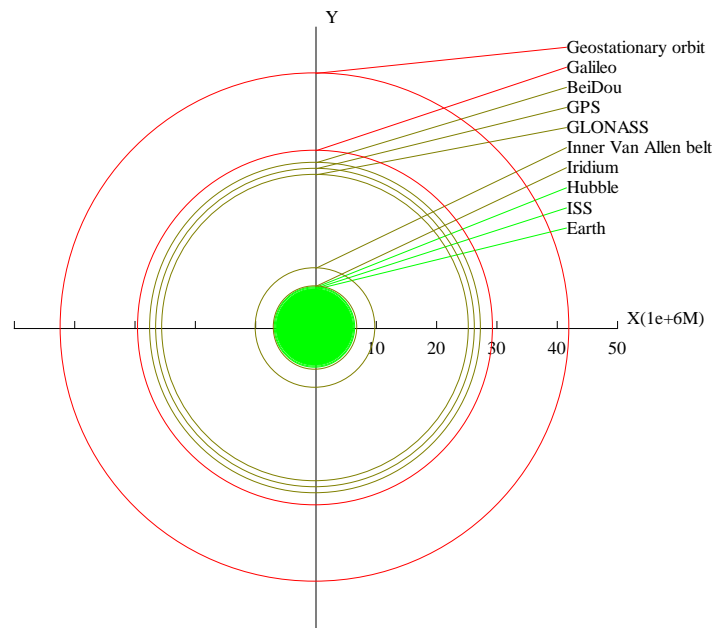


Fig.9 Orbit size comparison of Earth; ISS; Hubble; Iridium; Inner Van Allen belt; GLONASS; GPS; BeiDou; Galileo; Geostationary orbit. The Moon's orbit is around 9 times as large as geostationary orbit.

```
<Clet2020 Script>/[26]
char str[200]; int i,j,k,nP[10];double r,x,y,z,c,D[220];
char Satellite[200]="Earth;ISS;Hubble;Iridium;Inner Van Allen belt;GLONASS;GPS;BeiDou;Galileo;Geostationary orbit;";
double sr[20]={6.4,6.6,6.8,7,10,25.5,26.5,27.5,29.5,42.2,};
main(){ x=1;y=2*x+1;//Format(str,"x=%f y=%oe",x,y);
SetAxis(X_AXIS,-50,0,50,"X(1e+6M); ; ; ; ; ; 10;20;30;40;50;");SetAxis(Y_AXIS,-50,0,50,"Y;");
DrawFrame(FRAME_SCALE,2,0xaffaf);
for(i=0;i<10;i+=1) {r=sr[i];D[0]=r;D[1]=-r;D[2]=r;D[3]=r;c=Colorize(0,1,i/10);
SetPen(1,c);nP[0]=ELLIPSE;nP[1]=0;nP[2]=2;nP[3]=XY;if(i==0) nP[1]=1;Draw(nP,D);
nP[0]=TAKE;nP[1]=i;nP[2]=0;TextJob(nP,Satellite,str);x=750;y=400-i*20;TextAt(x,y,str);
D[0]=500;D[1]=500-r*6;D[2]=x;D[3]=y;Draw("LINE,0,2,PX",D);
}}#v07=#t(click here to run)#v07?>A
```

8. Conclusions

It was found that ultimate acceleration can enhance the quantum gravity effects for test [28,30]. If there is an ultimate acceleration β , nobody's acceleration can exceed this limit β , in the solar system, $\beta=2.961520e+10(m/s^2)$. Because this ultimate acceleration is a large number, any effect connecting to β will become easy to test, including quantum gravity test. As an application, the quantum gravity theory with the ultimate acceleration provides a useful formula to calculate the space debris distribution around the earth, in this paper the calculation results agree well with the experimental observation which are a set of measurements by incoherent scattering radar of EISCAT in the Arctic circle. Using the same approach, the radius of the Sun is calculated out to be $r=7e+8$ (m) with a relative error 0.72%; the radius of the Earth is calculated out to be $r=6.4328e+6$ (m) with a relative error 0.97%.

References

- [1]C. Marletto, and V. Vedral, Gravitationally Induced Entanglement between Two Massive Particles is Sufficient Evidence of Quantum Effects in Gravity, *Phys. Rev. Lett.*, 119, 240402 (2017)
- [2]T. Guerreiro, Quantum effects in gravity waves, *Classical and Quantum Gravity*, 37 (2020) 155001 (13pp).
- [3]S. Carlip, D. Chiou, W. Ni, R. Woodard, Quantum Gravity: A Brief History of Ideas and Some Prospects, *International Journal of Modern Physics D*, V,24,14,2015,1530028. DOI:10.1142/S0218271815300281.
- [4]de Broglie, L., *CRAS*,175(1922):811-813, translated in 2012 by H. C. Shen in *Selected works of de Broglie*.
- [5]de Broglie, *Waves and quanta*, *Nature*, 112, 2815(1923): 540.
- [6]de Broglie, *Recherches sur la théorie des Quanta*, translated in 2004 by A. F. Kracklauer as *De Broglie, Louis, On the Theory of Quanta*. 1925.
- [7]NASA, <https://solarscience.msfc.nasa.gov/interior.shtml>.
- [8]NASA, <https://nssdc.gsfc.nasa.gov/planetary/factsheet/marsfact.html>.
- [9]B. Ryden *Introduction to Cosmology*, Cambridge University Press, 2019, 2nd edition.
- [10]D. Valencia, D. D. Sasselov,R. J. O'Connell, Radius and structure models of the first super-earth planet, *The Astrophysical Journal*, 656:545-551, 2007, February 10.
- [11]D. Valencia, D. D. Sasselov,R. J. O'Connell, Detailed models of super-earths: how well can we infer bulk properties? *The Astrophysical Journal*, 665:1413–1420, 2007 August 20.
- [12]T. Guillot, A. P. Showman, Evolution of "51Pegasus-like" planets, *Astronomy & Astrophysics*,2002, 385,156-165, DOI: 10.1051/0004-6361:20011624
- [13]T. Guillot, A. P. Showman, Atmospheric circulation and tides of "51Pegasus-like" planets, *Astronomy & Astrophysics*,2002, 385,166-180, DOI: 10.1051/0004-6361:20020101
- [14]L.N. Fletcher,Y.Kaspi,T. Guillot, A.P. Showman, How Well Do We Understand the Belt/Zone Circulation of Giant Planet Atmospheres? *Space Sci Rev*, 2020,216:30. <https://doi.org/10.1007/s11214-019-0631-9>
- [15]Y. Kaspi, E. Galanti, A.P. Showman, D. J. Stevenson, T. Guillot, L. Iess, S.J. Bolton, Comparison of the Deep Atmospheric Dynamics of Jupiter and Saturn in Light of the Juno and Cassini Gravity Measurements,*Space Sci Rev*, 2020, 216:84. <https://doi.org/10.1007/s11214-020-00705-7>
- [16]Orbital Debris Program Office, *HISTORY OF ON-ORBIT SATELLITE FRAGMENTATIONS*, National Aeronautics and Space Administration, 2018, 15 th Edition.

- [17]M. Mulrooney, The NASA Liquid Mirror Telescope, *Orbital Debris Quarterly News*, 2007, April,v11i2,
- [18]Orbital Debris Program Office, Chinese Anti-satellite Test Creates Most Severe Orbital Debris Cloud in History, *Orbital Debris Quarterly News*, 2007, April,v11i2,
- [19]A. MANIS, M. MATNEY, A. VAVRIN, D. GATES, J. SEAGO, P. ANZ-MEADOR, Comparison of the NASA ORDEM 3.1 and ESA MASTER-8 Models, *Orbital Debris Quarterly News*, 2021, Sept,v25i3.
- [20]D. Wright, Space debris, *Physics today*,2007,10,35-40.
- [21]TANG Zhi-mei, DING Zong-hua, DAI Lian-dong, WU Jian, XU Zheng-wen, "The Statistics Analysis of Space Debris in Beam Parking Model in 78° North Latitude Regions," *Space Debris Research*, 2017, 17,3, 1-7.
- [22]TANG Zhimei DING, Zonghua, YANG Song, DAI Liandong, XU Zhengwen, WU Jian The statistics analysis of space debris in beam parking model based on the Arctic 500 MHz incoherent scattering radar, *CHINESE JOURNAL OF RADIO SCIENCE*, 2018, 25,5, 537-542
- [23]TANG Zhimei, DING, Zonghua, DAI Liandong, WU Jian, XU Zhengwen, Comparative analysis of space debris gaze detection based on the two incoherent scattering radars located at 69N and 78N, *Chin . J . Space Sci*, 2018 38,1, 73-78.
DOI:10.11728/cjss2018.01.073
- [24]DING Zong-hua, YANG Song, JIANG hai, DAI Lian-dong, TANG Zhi-mei, XU Zheng-wen, WU Jian, The Data Analysis of the Space Debris Observation by the Qijing Incoherent Scatter Radar, *Space Debris Research*, 2018, 18,1, 12-19.
- [25]YANG Song, DING Zonghua, Xu Zhengwe, WU Jian, Statistical analysis on the space posture, distribution, and scattering characteristic of debris by incoherent scattering radar in Qijing, *Chinese Journal of Radio science*, 2018 33,6 648-654,
DOI:10.13443/j.cjors.2017112301
- [26]Clet Lab, Clet: a C compiler, <https://drive.google.com/file/d/1OjKqANcgZ-9V56rgcoMtOu9w4rP49sgN/view?usp=sharing>
- [27]Huaiyang Cui, Relativistic Matter Wave and Its Explanation to Superconductivity: Based on the Equality Principle, *Modern Physics*, 10,3(2020)35-52. <https://doi.org/10.12677/MP.2020.103005>
- [28]Huaiyang Cui, Relativistic Matter Wave and Quantum Computer, Kindle ebook, 2021.
- [29]Huaiyang Cui, Evidence of Planck-Constant-Like Constant in Five Planetary Systems and Its Significances, *viXra*:2204.0133, 2022.
- [30]Huaiyang Cui, Approach to enhance quantum gravity effects by ultimate acceleration, *viXra*:2205.0053, 2022.
- [31]N.Cox, *Allen's Astrophysical Quantities*, Springer-Verlag, 2001, 4th ed..